

## Evaluation of Hardness and Fracture Toughness in a Porcelain Stoneware with Pseudoboehmite Additions

O. Aguilar-García\*, S. Bribiesca-Vazquez and J. Zárate-Medina

Instituto de Investigaciones Metalúrgicas, UMSNH, Edificio U, Ciudad Universitaria, Apdo. Postal 888, C.P. 58000, Morelia, Michoacán, México.

The effect of pseudoboehmite additions to conventional stoneware porcelain is investigated. Green compacts were formed by slip casting of stabilized aqueous suspensions and then sintering at 1,150 °C, 1,200 °C and 1,250 °C. The phase evolution was followed by XRD, the densification degree was calculated from densities and the microstructures were studied by SEM. Hardness,  $H$  and fracture toughness,  $K_{IC}$  were measured by Vicker's indentation. When vitrification occurs the presence of the pseudoboehmite leads to a extra mullitization, which has two consequences: a volume expansion resulting in a high porosity and a decrease of the amount of liquid which causes problems with the densification, by these facts the pseudoboehmite particles decrease the fracture toughness of the bodies.

**Key words:** Mechanical properties, Indentation, Mullite, Pseudoboehmite.

### Introduction

Although extensive work has been done related to the processing and characterization of porcelain, the accelerated growth rate of the global production of this type of material create the necessity of enhancement in the mechanical properties [1].

Porcelain stonewares are primarily composed of clay, feldspar and quartz, heat-treated to form a mixture of glass and crystalline phases. Composition variations are negligible and can be represented graphically as a portion of the  $(Na_2O, K_2O)-Al_2O_3-SiO_2$  phase diagram. Most of the reactions occurring during firing are kinetically-governed processes that do not reach thermodynamic equilibrium, since the industrial cycles are very short. Hence, it is very common for the finished product to contain crystals of quartz and feldspars that have not been entirely transformed.

Alumina has been introduced into the classic triaxial porcelain body composition to replace some of the feldspar and flint in order to improve its mechanical properties. Much has been written to clarify why the incorporation of alumina into porcelain bodies produces a strength increase [2]. However, the theories remain controversial. Although some authors attribute the increase in strength to the increase in the mullite content associated with a decrease in the quartz content, others have found no relationship between mechanical strength and mullite content [3].

Hardness testing is the most frequently used method for characterizing mechanical properties of ceramics. An indenter

of a well-defined geometry is pressed into the surface of the sample under a predefined load [4]. The quotient of the load and the area of the residual indentation impression are regarded as the measure of hardness. The Vickers indentation test is a common method used to characterize the hardness of materials. These experiments are simple to perform, need a small quantity of material, are generally non-destructive and can be repeated many times [5-9].

The measurements of fracture toughness of glasses and ceramics are complicated because of the very high brittleness of these materials. Sample preparation is time consuming and expensive. Methods, based on single edge notched beam (SENB, ASTM STP 1419), single edge precracked beam (SEPB, ISO 15732), the single 389 edge V-notched beam (SEVNB, CEN/TS 14425-5:2004), Chevron notched beam, surface crack in flexure (CNB and SCF, ASTM C1421-01b) and other conventional techniques require very precise notch geometry control. Results crucially depend on the surface preparation and on the state of residual stresses. On the other hand, the indentation fracture toughness technique is much easier to conduct. There is no need for the preparation of specimens with a special geometry and complex notches. Method involves measurements of the lengths of the cracks, which emanate from the corners of Vickers indentation diagonals, of the applied indentation load and of a few material properties such as elastic modulus.

Various equations are proposed in order to determine the fracture toughness from Vickers indentation cracks for both crack geometries. In this paper we compare different IFT measurement methods for porcelain stoneware.

It is well known that, both  $H$  and  $K_{IC}$ , depend on the microstructure, which is strongly influenced by the processing and heating schedule. The aim of the present

\*Corresponding author:  
Tel : +52 (443) 316 8355  
Fax: +52 (443) 327 5543  
E-mail: omarag@mail.com

study is to investigate the variation of the  $H$  and  $K_{IC}$  mechanical parameters as a function of the microstructures of the porcelain samples. These bodies had particles of pseudoboehmite added and their toughening mechanisms analyzed.

## Materials And Methods

### Raw Materials

The starting materials were nepheline sianyte (48 wt%), kaolin (30 wt%), ball clay (10 wt%) and quartz sand (12 wt%). Additions of pseudoboehmite were made to the batch of porcelain; the pseudoboehmite was obtained using the U. G (Universidad de Guanajuato) process of the alunite [10]. The averages particles sizes of the feldspar, kaolin, ball clay, quartz sand and pseudoboehmite used are 2.41, 1.43, 1.36, 5.92 and 0.5  $\mu\text{m}$ , respectively.

### Sample Preparation

Typical industrial porcelain stoneware was modified with additions of pseudoboehmite. Suspensions of mixtures of porcelain and pseudoboehmite particles were prepared always at a solid loading of 69 wt%. The dispersion conditions were achieved using a mixture of defloculants (darvan 7, darvan 811 and sodium silicate) [11] while the slip was being mechanically stirred. The slip was transferred to a plastic container and aged for at least a week before any casting was carried out. Disc specimens with dimensions of  $100 \times 10$  mm were cast by a conventional technique and dried at  $110^\circ\text{C}$  for 24 h. The discs were produced with three different content of pseudoboehmite particles (2, 5, 10 wt%) were fired in an electric furnace at a heating rate of  $10^\circ\text{K minute}^{-1}$  until they reached a temperature of between 1,000 and 1,250  $^\circ\text{C}$  with a soaking time of 2 h.

### Measurements and analysis

The bulk density of the green body was calculated using the weight and dimensions. The bulk density of the fired body was determined by water immersion, based on ASTM C20. The microstructure of the fired bodies was studied by means of scanning electron microscopy (SEM) using a JEOL JSM-6300 apparatus. Crystalline phases present in fired bodies were determined by X-ray diffraction by using a Siemens 5000 equipment with CuK radiation at 35 kV and 15 mA. The samples for SEM observation were polished and etched with hydrofluoric acid to dissolve the glassy matrix and enhance the crystalline morphologies.

The hardness ( $H$ ) and the fracture toughness ( $K_{IC}$ ) were

**Table 1.** Selected equations for  $K_{IC}$  measurements with Vicker's indentations

No.Ref.	Radial-Median type crack system	Palmqvist type crack system
1	$0.0303(H_v a^{1/2})(E/H_v)^{2/5} \log(8.4a/c)$	
2	14	$0.0782(H_v a^{1/2})(E/H_v)^{2/5} (c/a)^{-1.56}$
3	15	$0.009052(H_v^{3/5})(E^{2/5})(a)(c^{1/2})$
4	13	$0.0495(H_v a^{1/2})(E/H_v)^{2/5} (c/a)((c/18a)-1.51)$

measured (Mitutoyo MVK-E3 tester) by Vickers indentation on the polished surfaces of the sintered samples (diamond pastes of 6, 3 and 1  $\mu\text{m}$ ).

Vickers hardness measurements  $HV_{0.05}$ ,  $HV_{0.1}$ ,  $HV_{0.2}$ ,  $HV_{0.3}$ ,  $HV_{0.5}$  and  $HV_1$ , were performed according to ISO 6507, using indentation loads: 0.49035 N (0.05 kgf), 0.9807 N (0.1 kgf), 1.961 N (0.2 kgf), 2.943 N (0.3 kgf), 4.903 N (0.5 kgf) and 9.807 N (1 kgf) respectively. Indentation tests were carried under laboratory conditions.  $H$  was calculated from  $H = 1.8544L/a^2$  ( $L$ : indentation load [N] and  $a$ : Vickers dimension or semidiagonal [ $\mu\text{m}$ ]).

For fracture toughness the samples were submitted to 10 loads of 9.8 N for 15 s on each indentation. The cracks were measured using the microscope attachment on the microhardness tester immediately after indentation. Crack measurements were only made on indents that were well defined without chipping and for which the cracks did not terminate at pores. The indentation fracture toughness of the material was evaluated selecting four models commonly

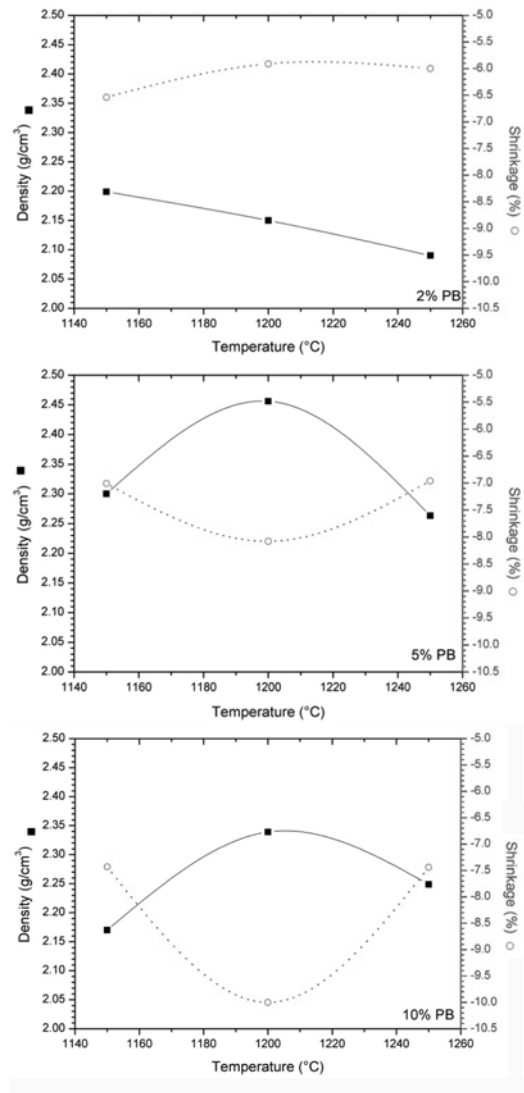


**Fig. 1.** Densification and shrinkage behavior of the porcelain with different PB additions.

used in ceramic studies (table 1); model 1 considers that the emanating indentation cracks are radial-medial type, model 2 and 3 correspond to a Palmqvist crack system and finally model 4 is a formulation adjusting any type of indentation crack system. These models are presented in table 1, where P corresponds to the applied load of indentation (N), c the crack length (mm), a the indent length (mm), Hv the Vickers hardness (GPa) and E the Young's modulus of the material (GPa).

In order to use the dedicated equations for the calculation of fracture toughness it is necessary to have a value of Young's modulus which was measured by the impulse excitation technique (Grindo-Sonic, J. W. Lemmens Inc.)

## Results And Discussion

### Crystalline phases and densities

The densification behaviors of the samples are shown in the fig. 1 Porcelain with an addition of 2% of PB (fig. 1(a)), shows a maximum densification at around 1,150 °C and then decreases. The decrease in density after reaching the maximum is attributed to bloating. The addition of PB into the batch of porcelain affects the sintering behavior as we can see in figs. 1(b) and (c), further increasing the PB content in the batch caused a significant increment of shrinkage and density at 1,200 °C, this can be attributed to the excess of OH groups caused by the additions of pseudoboehmite and the increment in the mullite phase into the batch respectively. After reaching the maximum densification the samples show a decrease, this is attributed to a volume expansion associated with the reaction of the mullite. The lack of densification and the increment of porosity at high temperatures and with the additions of PB (fig. 2) corresponds to intense mullitization. Other authors have noticed the detrimental effect of mullitization on the densification in other materials [16-17]; in alumina-zircon mixtures this has been attributed to a volume

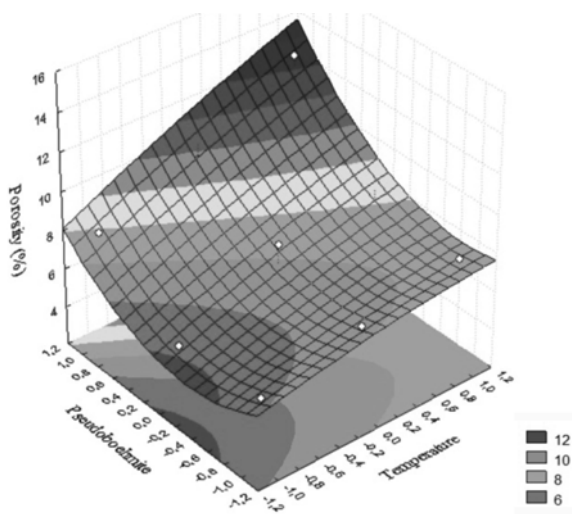


**Fig. 2.** Variation of the porosity as a function of the temperature and PB additions.

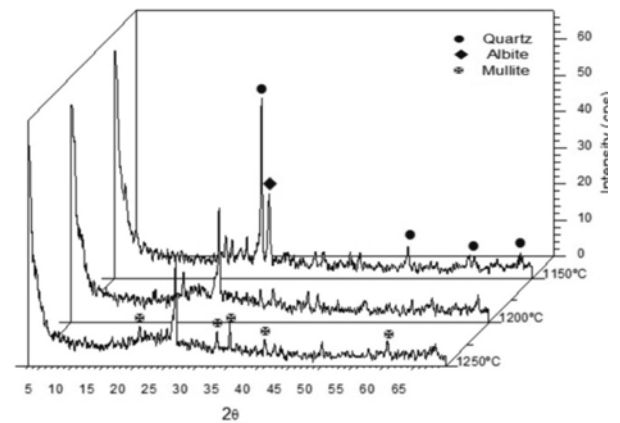


**Fig. 3.** XRD of porcelain stoneware containing 2 wt% of pseudoboehmite.

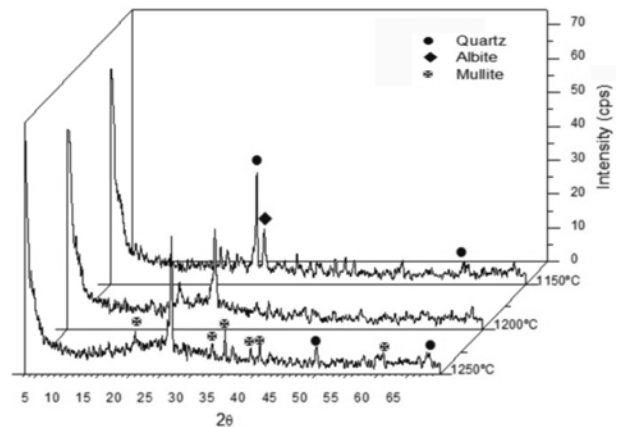


**Fig. 4.** XRD of porcelain stoneware containing 5 wt% of pseudoboehmite.

expansion associated with the reaction [18]. In this study it has been shown that the increment in the mullite phase can be correlated with the high porosity present in the mixture of the porcelain with an increment of the addition of PB.

XRD from the samples with 2% of particles of pseudoboehmite (PB) reinforcement fired at 1,15 °C, 1,200 °C and 1,250 °C are presented in fig. 3. Albite melted, leading to loss of crystal peaks at 1,200 °C and 1,250 °C, respectively. Melting was followed by the appearance of a hump indicating that a viscous liquid formed and cooled to a glass. Mullite peaks increased in intensity with the firing temperature, whereas quartz peaks decreased, this is associated with the partial dissolution of  $\alpha$ -quartz. The samples that contain a 5% of PB shows an increment of the mullite phase with respect to the porcelain with 2% (fig. 4); this suggests that the fluxing action of the feldspar, the amorphous silica from clay relicts during meta-kaolin formation with the addition of Al from the pseudoboehmite particles facilitated crystallization of mullite more than in the porcelain with 2% of PB. The decreased intensity of the  $\alpha$ -quartz peaks at > 1,200 °C showed the partial dissolution of  $\alpha$ -quartz at higher temperatures, no cristobalite was present. Samples from the batch containing 10% of

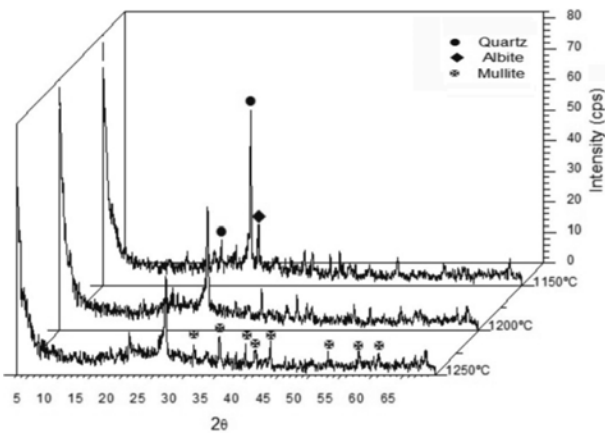


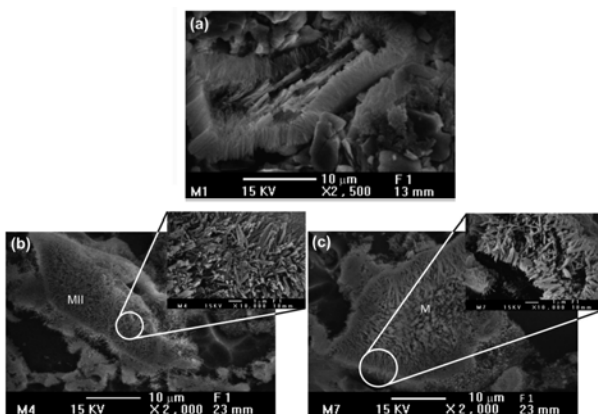
**Fig. 5.** XRD of porcelain stoneware containing 10 wt% of pseudoboehmite.

PB (fig. 5) showed a quite different evolution as revealed by XRD were mullite peaks increase in intensity, this could be happening because of the high reactivity of the particles of pseudoboehmite. As we can see in the fig. 5 the lack of liquid/glassy phase in the sample with 10% of PB is induced by an extra mullitization and explains why the quartz dissolution and final densification are limited in this material.

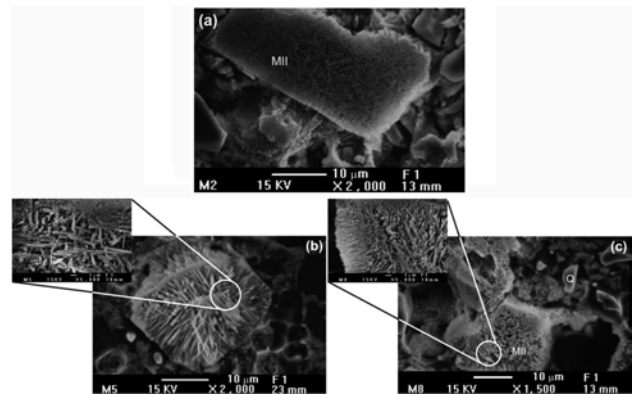
### Microstructures

Fig. 6(a) is a SEI of a sample with 2% of PB fired at 1,150 °C, showing the typical microstructure of a commercial porcelain stoneware[19]. Cuboidal mullite crystals, smaller in size, are not necessarily MI, this is because they are aligned along [001] so their lengths and their aspect ratio cannot be determined. Elongated secondary mullite crystals (< 2 μm) can be observed even at 1,150 °C. By rising the sintering temperature, the amount of more homogeneous elongated crystals of mullite secondary (~ 2 μ long) also increase (fig. 6(b), (c)).

In fig. 7(a) the quartz particles remain angular, although the presence of minor solutions rims indicates some dissolution. Other features are a glassy phase and secondary



**Fig. 6.** SEM/secondary electron images of samples containing 2% of PB fired at (a) 1,150 °C, (b) 1,200 °C and (c) 1,250 °C.



**Fig. 7.** SEM/secondary electron images of samples containing 5% of PB fired at (a) 1,150 °C, (b) 1,200 °C and (c) 1,250 °C.

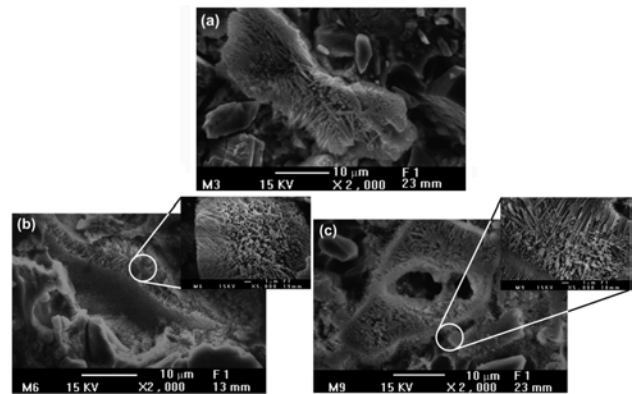


**Fig. 8.** SEM/secondary electron images of samples containing 10% of PB fired at (a) 1,150 °C, (b) 1,200 °C and (c) 1,250 °C.

mullite. The sample fired at 1,200 °C shows a more elongated crystal of secondary mullite (~ 5 μm). At 1,250 °C the length of crystals of secondary mullite appears to be the same, but in a denser and more homogeneous distribution. Fig. 7(c) reveals clear quartz solution rims and more rounded than angular particles of quartz.

The microstructure seen in the fig. 8(a) shows angular α-quartz crystals indicating that α-quartz dissolution had not yet begun; at 1,250 °C (fig. 8(c)) rounding of the edges of the α-quartz crystal indicated their partial dissolution. Formation and recrystallization of acicular type secondary mullite are therefore facilitated in the composition that contains higher amounts of pseudoboehmite and this is evident in the figs. 8(a-c). This is a consequence of the high reactivity of the pseudoboehmite particles that are dissolved by the glass and consequently precipitate as a mullite phase. The elongated crystals (3 μm long and 0.4 μm of wide) in fig. 8(b) were identified as secondary mullite. With the increment of the temperature (fig. 8(c)) the lengths of the mullite crystals grow but its width remains equal (≤ 5 μm long and 0.5 μm wide).

The main difference between the nine materials is the amount of mullite produced. The presence of any type of alumina that could remain inert in the porcelain was not

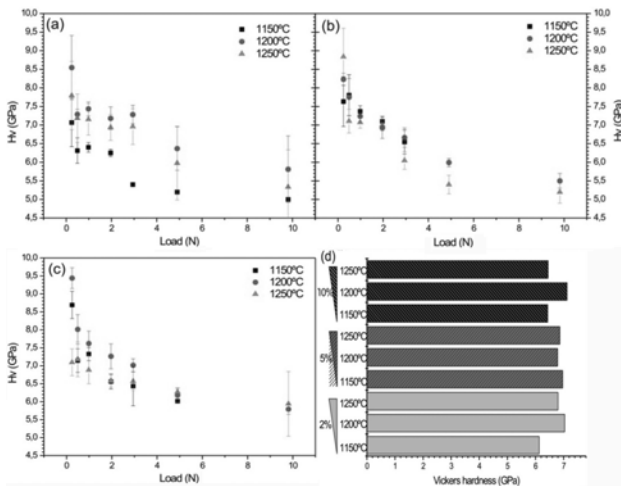


**Fig. 9.** Vicker's hardness as a function of the application load of batches of porcelain with (a) 2 %wt of PB, (b) 5%wt of PB, (c) 10%wt of PB and (d) Vicker's hardness as a function of the composition of the material and the temperature.

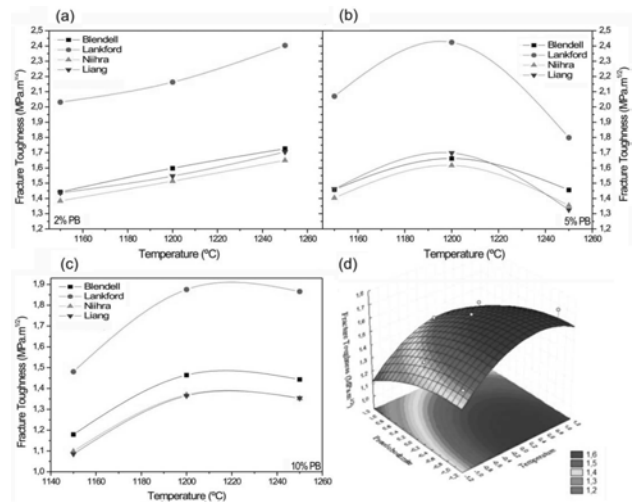


**Fig. 10.** Variation of the fracture toughness obtained with the different formulations with (a) 2% of pseudoboehmite, (b) 5% of PB, (c) 10% of PB and (d) surface graphic using the Blendell model.

**Table 2.** Physical properties of the porcelain with different PB additions

PSEUDO-BOEHMITE(%)	TEMPERATURE(°C)	SAMPLE	BULK DENSITY(g/cm <sup>3</sup> )	POROSITY(%)	SHRINKAGE(%)
2	1,150	1	2.07	5.6	6.54
	1,200	4	2.009	6.6	5.91
	1,250	7	1.93	7.62	6
5	1,150	2	2.18	5.09	7.01
	1,200	5	2.23	7.82	8.08
	1,250	8	2.092	7.54	6.96
10	1,150	3	2.001	7.99	7.43
	1,200	6	2.119	9.4	10
	1,250	9	1.965	12.62	7.44

detected and for this fact we conclude that the particles of pseudoboehmite can be dissolved by the glass and so the mullite precipitates. This phenomenon occurs at high temperatures in alumina-rich porcelains [19], but in the present study this occurs at a lower temperature because of the reactivity of the particles of the pseudoboehmite.

**Hardness and fracture toughness**

The hardness dependence on indentation load was determined for all materials, which were fired at three different temperatures (figs. 9(a-c)) in order to establish the load from which the hardness can be considered constant. Data points represent an average measurement from at least ten tests. The hardness (H) decreased to a constant value when increasing the load up to 1.961 N. At lower loads, the high dependence of H on the indentation load is observed in every material studied. The variation of hardness as a function of the composition of the materials for the different thermal cycles is shown in fig. 9(d). The hardness for all the materials shows an increment at 1,200 °C and then a decrease at 1,250 °C, this could be attributed to the densification of the material. The hardness is higher with the additions of PB which may be associated with

the mullite content in the porcelain and the reduction of the vitreous phase.

The results of the indentation fracture toughness calculated with the different models are shown in the fig. 10(a-c). In general all the models, except for the model proposed by Lankford, are in agreement with the expected values of this type of material which are in the range of 1-1.6 MPa.m<sup>1/2</sup> [20-22]. The fracture toughness showed some variation both with sintering temperature and pseudoboehmite additions (fig. 10(d)). An analyses of the parameter interaction lead to the following deductions: (i) the most important synergistic interaction is that between the sintering temperature at 1,200 °C and a 5% of addition of PB, this is consequence of the highest density of the sample and the decrease in the porosity, (ii) high additions of PB promote extra mullitization with two main consequences: the first is the modification of the liquid phase that makes the process of sintering more difficult and consequently the densification and second the promotion of gases attributed to the elimination of OH groups of the pseudoboehmite and the volume expansion associated with the reaction that originate the mullite, these factors developed an increase in the porosity and consequently a decrease in the fracture toughness.

## Conclusions

The densification is suppressed with high additions of pseudoboehmite particles, since shrinkage is inhibited and the amount of glassy phase is reduced.

The addition of pseudoboehmite particles into the porcelain promotes extra mullitization that has two main consequences. (i) a volume expansion associated with the reaction and (ii) an increment in the porosity attributed to the elimination of the OH groups of the pseudoboehmite and an increment of the viscosity of the glassy phase.

The mechanical response depends both on the initial composition and the sintering schedule. The highest densification and value of  $K_{IC}$  were obtained at 1,200 °C with 5% wt of addition of pseudoboehmite; this is a consequence of the quantity of crystalline phases and the low porosity.

The hardness values of porcelain samples presented in this paper are directly connected to their microstructures which vary according to the mineral composition of the raw materials and the firing temperature. We can see that the highest hardness is achieved at 1,200 °C when the samples have their highest densities. It was also noticed, that the most reliable results occur with loads of 1.96 N.

## Acknowledgment

The authors would like to acknowledge the financial support of CONACYT.

## References

1. T. Cavalcante, M. Dondi, G. Ercolani, G. Guarini, C. Melandri, M. Raimondo and E. Rocha, *Ceram. Int.*, 30 (2004) 953-963.
2. Z. Ke, *Am. Ceram. Soc. Bull.*, 69 (1990) 380-390.
3. E. De Los Monteros, D. Alvarez-Estrada and R. Martinez-Caceres, *Bol. Soc. Esp. Ceram. Vidrio*, 30[4] (1991)11-17.
4. D. Quinn, *J. Am. Ceram. Soc.*, 90[3] (2007) 673-680.
5. R. Lawn, T.R. Wilshaw, *J. Mater. Sci.*, 10 (1975) 1049-1081.
6. R. Lawn, G. Evans and B. Marshall, *J. Am. Ceram. Soc.*, 63 (1980) 574-581.
7. R. Anstis, P. Chantikul, R. Lawn and B. Marshall, *J. Am. Ceram. Soc.*, 64 (1981) 533-538.
8. K. Shetty, R. Rosenfield and H. Duckworth, *J. Am. Ceram. Soc.*, 68 (1985) C282-284.
9. T. Laugier, *J. Mater. Sci. Lett.*, 6 (1987) 355-356.
10. H. Juarez, M. Martinez and M. Ruvalcaba, in *IV Congreso Iberoamericano de Quimica Inorganica*, Guanajuato, Gto., Mexico, 9 (1999) 483-489.
11. O. Aguilar, Phd Report, Universidad Michoacana De San Nicolas De Hidalgo, (2007) p35.
12. J. Blendell, Phd Thesis, Massachusetts Institute Of Technology, Cambridge, Ma, (1979).
13. M. Liang, R. Torrecillas, G. Orange and G. Fantozzi, *J. Mater. Sci.*, 25[12] (1990) 207-214.
14. J. Lankford, *J. Mater. Sci. Lett.*, 1[11] (1982) 493-495.
15. K. Niihara, *J. Mater. Sci. Lett.*, 2 (1983) 221-223.
16. C. F. Chan and Y.C. Ko., *Ceram. Int.*, 20 (1994) 31-37.
17. B. Saruhan, U. Voss and H. Schneider, *J. Mater. Sci.*, 29 (1994) 3261-3268.
18. V. Yaroshenko and D.S. Wilkinson, *J. Am. Ceram. Soc.*, 84[4] (2001) 850-858.
19. Y. Iqbal and W.D. Lee, *J. Am. Ceram. Soc.*, 80[12] (2000) 3121-3127.
20. F. Batista, F. Messer and J. Hand, *British Ceramic Transactions*, 10[6] (2001) 256-259.
21. R. Braganca, P. Bergmann, *Ceram. Int.*, 29 (2003) 801-806.
22. W.D. Callister, in "Materials Science and Engineering" (John Wiley & Sons Press, New York, 2000) p. A7.